Lithium Phosphoranylidene Carbenoids Mes*-P(═E)═C(X)Li(THF)$_3$ (E = NMes*, C(SiMe$_3$)$_2$; X = Br, Cl, F): Synthesis and Structural Investigations in Solution and Solid State

Thomas Baumgartner, Dietrich Gudat,* Martin Nieger, Edgar Niecke,* and Thomas J. Schiffer

Contribution from the Anorganisch-Chemisches Institut der Universität, Gerhard-Domagk-Strasse 1, D-53121 Bonn, Germany

Received January 8, 1999

Abstract: Phosphoranylidene carbenoids Mes*-P(═E)═C(X){Li(THF)$_3$} (E = C(SiMe$_3$)$_2$, NMes*; X = F, Cl, Br, **10**−**13**, **15**) were synthesized and their molecular structures characterized by low-temperature X-ray diffractometry and multinuclear NMR studies. The experiments confirm the presence of monomeric molecules with THF-solvated metal atoms in both solution and solid state. The solid carbenoids display elongated C−X bonds and distortions of carbon bond angles which represent typical features of carbenoids and suggest an interpretation of the bonding situation as a contact ion pair between a carbanion and a solvated metal cation. This is corroborated by NMR studies which show that the dynamic exchange between the two components in solution can be directly monitored in 2D ^{6}Li,^{31}P shift correlations. While structural and spectroscopic data give no evidence for a continuously increasing stability between F-, Cl-, or Br-substituted carbenoids, they reveal the presence of marked structural differences between the *E/Z*-isomers **10** and **15**. As is shown by 2D ^{6}Li,^{31}P NMR spectra, this deviation is accompanied by a noticeable difference in kinetic stabilities, which is assigned to be the cause for the known different reaction behavior of both isomers.

Introduction

Carbenoids[1] are well established in organic chemistry since the pioneering work of Köbrich and co-workers.[2−8] The special features of these compounds comprise the presence of both an electronegative element and a metal at the same carbon atom. This leads to a unique bonding situation with a "chameleon-like" ambident character for this carbon atom, as specified by the canonical structures **A**−**C** (Scheme 1). As a consequence of the different substituent electronegativities, the carbon−metal bond should exhibit high s-character and the carbon−halogen bond high p-character.[9] Similar considerations hold also for vinylidene derivatives, where the carbenoid center is an sp^2-hybridized carbon atom that is part of a double bond.[10] In connection with their ambident character, carbenoids display a versatile reactivity which appears to be controlled by the nature of the electronegative substituent X. Thus, species with X = OR or NR$_2$ react predominantly as electrophiles with nucleophilic reaction partners. In contrast, compounds with X = halogen display as well reactions with electrophiles[11] and have been widely used as valuable synthons in "umpolung" reactions with carbonyls and related C−C-coupling reactions. Recently, the application of chiral carbenoids in stereoselective synthesis has been reported.[12]

Scheme 1

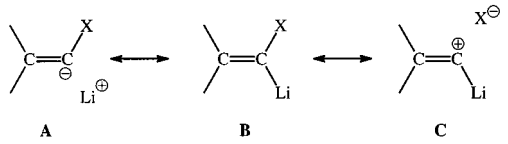

Since the presence of two leaving groups of opposite polarity at one carbon not only leads to enhanced reactivity but also facilitates fragmentation reactions, carbenoids are generally thermolabile and can exist only at low temperatures. The first experimental characterization of carbenoids was performed by Seebach et al.[13,14] in the early 1980s, and the reported low-temperature NMR data were considered to confirm predictions derived from quantum chemical studies.[15] Only recently, Boche et al.[16] reported in an exciting piece of work that carbenoids can be obtained as isolable species which can be structurally

* Address correspondence to these authors. Telefax: Int.-228−73 53 27. E-mail: e.niecke@uni-bonn.de; dgudat@uni-bonn.de.

(1) Stang, P. J. In *Methods of Organic Chemistry (Houben Weyl)*, 4th ed.; Regitz, M., Ed.; Thieme: Stuttgart, 1989; Vol. E, 19b, pp 85−135.
(2) Köbrich, G.; Trapp, H. *Z. Naturforsch.* **1963**, *18b*, 1125−1128.
(3) Köbrich, G.; Büttner, H. *J. Organomet. Chem.* **1964**, *18*, 117−119.
(4) Köbrich, G.; Merkle, H. R.; Trapp, H. *Tetrahedron Lett.* **1965**, 969−972.
(5) Köbrich, G.; Trapp, H. *Chem. Ber.* **1966**, *99*, 670−680.
(6) Köbrich, G.; Goyert, W. *Tetrahedron* **1967**, *22*, 2621.
(7) Köbrich, G.; Heinemann, H.; Zünndorf, W. *Tetrahedron* **1967**, *23*, 565−570.
(8) Köbrich, G. *Angew. Chem.* **1967**, *79*, 15−27; *Angew. Chem., Int. Ed. Engl.* **1967**, *6*, 41−53.
(9) Lambert, C.; Schleyer, P. v. R. In ref 1, pp 15−19.
(10) Stang, P. J. *Chem. Rev.* **1978**, *78* 345−363.
(11) Braun, M. *Angew. Chem.* **1998**, *110*, 444−465; *Angew. Chem., Int. Ed. Engl.* **1998**, *37*, 430−451.
(12) Siegel, H. J. *Top. Curr. Chem.* **1982**, *106*, 55−78.
(13) Seebach, D.; Siegel, H.; Gabriel, J.; Hässig, R. *Helv. Chim. Acta* **1980**, *63*, 2046−2053.
(14) Seebach, D.; Hässig, R.; Gabriel, J. *Helv. Chim. Acta* **1983**, *66*, 308−337.
(15) Schleyer, P. v. R.; Clark, T.; Kos, A. J.; Spitznagel, G. W.; Rohde, C.; Arad, D.; Houk. K. N.; Rondan, N. G. *J. Am. Chem. Soc.* **1984**, *106*, 6467−6475.
(16) Boche, G.; Marsch, M.; Müller, A.; Harms, K. *Angew. Chem.* **1993**, *105*, 1081−1082; *Angew. Chem., Int. Ed. Engl.* **1993**, *32*, 1032−1033.

10.1021/ja990074e CCC: $18.00
Published on Web 06/11/1999

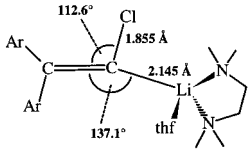

1

Figure 1. Selected structural parameters of the vinylidene carbenoid **1** (Ar = 4-chlorophenyl; data from ref 16).

Scheme 2

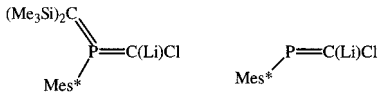

Mes* = 2,4,6-*t*Bu$_3$C$_6$H$_2$

characterized by X-ray diffractommetry. The structural parameters of the vinylidene derivative **1** (Figure 1) reveal a most peculiar distorted trigonal geometry of the carbenic C1 atom with a large C2−C1−Li (137.1°) and a small C2−C1−Cl angle (112.6°), which confirmed the anticipated unequal distribution of s- and p-character between the C−Cl and C−Li bonds.[9] Distortions very similar to those described here have been previously noted for some chloroenamines[17] and ester enolates,[18] where they have been used in the context of the structure correlation principle[19] to predict the path of the fragmentation of the enolates into ketenes and alcoholates. In the course of our work on systems with P−C π-bonds, we recently succeeded in isolating a first methylenephosphoranylidene carbenoid, **2** (Scheme 2), in crystalline form.[20] The incorporation of the carbenoid center into a polar heteroallylic π-system appeared to add significantly to the stability of this molecule. This finding motivated us to attempt the synthesis and structural characterization of further phosphavinylidene carbenoids and conduct a systematic study of their structural and spectroscopic properties as well as their dynamic behavior in solution. Here, we report on syntheses, NMR data, and X-ray structure analyses of a series of lithiated imino- and methylenephosphoranylidene carbenoids with structures similar to **2**, including the first fluorocarbenoid, whose preparation was considered impossible until recently.[21] The comparison of structural and spectroscopic parameters allows us to analyze systematically the influence of the nature of the halogen substituent, the double bond configuration, and the modification of the delocalized π-system on the structural and spectroscopic parameters of the carbenoid functionality. Prior to the research described in this paper, we succeeded as well in the structural characterization of an analogue, phosphorus(III) vinylidene carbenoid **3** (Scheme 2).[22]

Results

Preparation and Characterization of C-Functionalized Bisylene Phosphorane Precursors. As shown previously, the bisylene phosphoranes **6** and **9**, which are suitable precursors for the corresponding chlorocarbenoids, are conveniently accessible via oxidation of the phosphaalkene **4**[23] or the iminophosphine **5**[24] with a sulfur ylide[25] or dichlorocarbene (Scheme 3).[20,26] The attempt to extend this route to prepare the dibromomethylene compound **7** by treatment of **4** with bromoform and *n*-butyllithium produced only a 10% yield of the desired product. A more satisfactory approach was found in a modified reaction scheme which involved the use of potassium *tert*-butoxide as base and afforded **7** in 90% yield. The formal oxidation of **4** by a chlorofluorocarbene moiety was achieved by addition of a mixture of **4** and $CFCl_3$ to a titanium(0) suspension.[27] Crude **8** (yield 97%) was obtained as a yellow oil after extraction with pentane, filtration, and removal of the solvent and was used without further purification. The novel products **7** and **8** were characterized by multinuclear NMR data, and the constitution of **7** was further confirmed by a single-crystal X-ray diffraction study.[28] Compound **7** displays a single set of resonances attributable to the bisylene phosphorane moiety (δ^{31}P, 136.9; δ^{13}C, 57.3 (^1J(P,C) = 120.9 Hz, CBr_2), 60.2 (^1J(P,C) = 48.5 Hz, C(SiMe$_3$)$_2$)). The NMR spectra of **8** display two sets of signals, indicating the presence of a mixture of *E/Z*-isomers in a ratio of 95:5. The fluorine substituent induces a shift of the ^{31}P NMR signals to higher field (δ^{31}P, 94.8 (^2J(P,F) = 40.7 Hz, major isomer), 92.3 (^2J(P,F) = 59.0 Hz, minor isomer)) as compared to those of **6** and **7** and introduces a marked difference between the shifts of the two methylene carbon atoms (δ^{13}C (major isomer), 135.7 (^1J(F,C) = 330.0 Hz, ^1J(P,C) = 165.2 Hz, CFCl), 44.3 (^2J(P,C) = 37.4 Hz, ^3J(F,C) = 8.0 Hz, C(SiMe$_3$)$_2$)).

Scheme 3

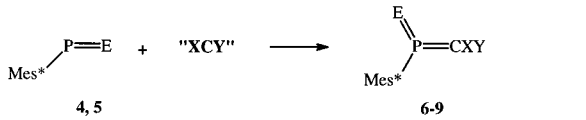

4, 5 **6-9**

4 E = C(SiMe$_3$)$_2$
5 E = NMes*

Mes* = 2,4,6-*t*Bu$_3$C$_6$H$_2$

6 E = C(SiMe$_3$)$_2$, X = Y = Cl
7 E = C(SiMe$_3$)$_2$, X = Y = Br
8 E = C(SiMe$_3$)$_2$, X = Cl, Y = F
9 E = NMes*, X = Y = Cl

Preparation of Imino- and Methylenephosphoranylidene Carbenoids. As previously reported,[20] reaction of the bisylene phosphorane **6** with 1 equiv of *n*-butyllithium in THF at −78 °C proceeded via X/Li exchange to give a mixture of the *Z*- and *E*-configured carbenoids **10** and **15** (molar ratio approximately 6:1) (Scheme 4). Extension of this protocol to the bisylene phosphoranes **7** and **9** afforded similar mixtures of two products, which were assigned to the stereoisomeric carbenoids **11**/**16** and **13**/**17**, respectively. The observed isomer ratio of 6:1 is similar to the one found during the metalation of **6**, suggesting that the regioselectivity of the Li/X exchange is governed by the steric accessibility of the reaction sites, and the observed products are formed under kinetic control. Metalation of the chlorofluoromethylene moiety in **8** proceeded exclusively via

(17) Seebach, D.; Amstutz, R.; Laube, T.; Schweizer, W. B.; Dunitz, J. D. *J. Am. Chem. Soc.* **1985**, *107*, 5403−5409.
(18) van Meerssche, M.; Germain, G.; Declercq, J. P.; Molhant, N. *Cryst. Struct. Commun.* **1979**, *8*, 45.
(19) Bürgi, H. B.; Dunitz, J. D. *Structure Correlation*; VCH: Weinheim, 1994; Vol. 2.
(20) Niecke, E.; Becker, P.; Nieger, M.; Stalke, D.; Schoeller, W. W. *Angew. Chem.* **1995**, *107*, 2012−2015; *Angew. Chem., Int. Ed. Engl.* **1995**, *34*, 1849−1852.
(21) Baumgartner, T.; Gudat, D.; Nieger, M.; Niecke, E., manuscript submitted.
(22) Schmidt, O.; Nieger, M.; Niecke, E.; Schoeller, W. W. *J. Am. Chem. Soc.* **1999**, *121*, 519−522.
(23) Cowley, A. H.; Jones, R. A.; Lasch, J. G.; Norman, N. C.; Stewart, C. A.; Stuart, A. L.; Atwood, J. L.; Hunter, W. E.; Zhang, H.-M. *J. Am. Chem. Soc.* **1984**, *106*, 7015−7020.
(24) Larbig, M.; Nieger, M.; von der Gönna, V.; Ruban, A. V.; Niecke, E.; *Angew. Chem.* **1995**, *107*, 505−507; *Angew. Chem., Int. Ed. Engl.* **1995**, *34*, 460−462.
(25) Baumgartner, T.; Schinkels, B.; Gudat, D.; Nieger, M.; Niecke, E. *J. Am. Chem. Soc.* **1997**, *119*, 12410−12411.
(26) Schilbach, W.; von der Gönna, V.; Gudat, D.; Nieger, M.; Niecke, E. *Angew. Chem.* **1994**, *106*, 1037−1038; *Angew. Chem., Int. Ed. Engl.* **1994**, *33*, 982−983.
(27) Dolbier, W. R., Jr.; Burkholder, C. R. *J. Org. Chem.* **1990**, *55*, 589−594.
(28) Baumgartner, T.; Nieger, M.; Niecke, E., unpublished results.

Table 1. Data on the Crystal Structure Solution and Refinement for **10**, **11**, and **13**

	10	**11**	**13**
formula	$[C_{26}H_{47}ClPSi_2]^-[Li(C_4H_8O)]^+$	$[C_{26}H_{47}BrPSi_2]^-[Li(C_4H_8O)]^+$	$[C_{37}H_{58}ClNP]^-[Li(C_4H_8O)]^+ - 2.5\ (C_4H_8O)$
cryst syst	monoclinic	monoclinic	triclinic
space group	$P2_1/n$ (No. 14)	$P2_1/n$ (No. 14)	$P\bar{1}$ (No. 2)
a, Å	13.5149(4)	13.5250(3)	13.0881(12)
b, Å	23.1607(4)	23.2920(5)	20.0075(18)
c, Å	13.5326(4)	13.5480(3)	24.901(2)
α, deg			74.184(6)
β, deg	90.061(1)	90.241(4)	79.562(7)
γ, deg			71.725(4)
V, Å^3	4235.9(2)	4267.9(2)	5924.5(9)
Z	4	4	4
ρ_{calc}, g cm^{-3}	1.11	1.17	1.11
μ	0.22	1.09	0.14
diffractometer	Nonius KappaCCD	Nonius KappaCCD	Nonius KappaCCD
radiation	Mo Kα	Mo Kα	Mo Kα
λ, Å	0.710 73	0.710 73	0.710 73
T, K	123(2)	123(2)	123(2)
max 2*θ*, deg	57.0	52.0	46.7
no. of data	31 249	23 067	31 439
no. of unique data	7962	6795	15 621
no. of unique data [$I > 2\sigma(I)$]	6120	5159	8897
no. of variables	443	416	1223
no. of restraints	235	0	3533
$R(F)^a$	0.038	0.054	0.103
w$R2(F^2)$ for all data	0.115	0.121	0.326

[a] For $I > 2\sigma(I)$.

Scheme 4

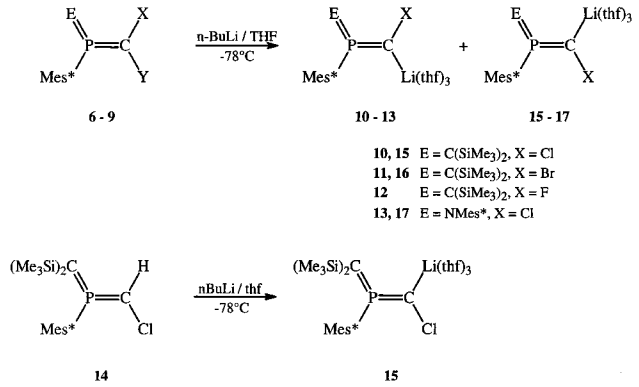

Li/Cl exchange and gave the *Z*-configured carbenoid **12** as the main product.[21] Formation of the corresponding *E*-isomer, which was anticipated on grounds of the presence of the appropriate precursor in the starting material, could not be unambiguously confirmed. The major products of all reactions were isolated as highly air- and moisture-sensitive crystals by crystallization at −50 °C and identified as carbenoids **10**−**13** with a *Z*-configuration at the metalated double bond by single-crystal X-ray diffractommetry. The described synthetic protocol allowed further preparation of ^{6}Li-doped samples of **10**−**13** for the purpose of NMR spectroscopic characterization, starting from the bisylene phosphoranes **6**−**9** and [^{6}Li]butyllithium. In addition, a ^{6}Li-doped sample of the *E*-carbenoid **15** was generated via Li/H exchange from **14** as reported previously.[20]

Crystal Structure Studies of 10, 11, and 13. Relevant data describing the crystal structures of the carbenoids **10**, **11**, and **13** are collected in Table 1. Solid **13** exhibits two crystallographically independent molecules with very similar geometric parameters in the asymmetric unit. The molecular structures of **10** (compounds **10** and **11** are isostructural) and one of the independent molecules of **13** are displayed in Figures 2 and 3. Important structural parameters are listed together with the corresponding data of **12**[21] and **15**[20] in Table 2. Similarly to the case of the previously characterized lithiated bisylene

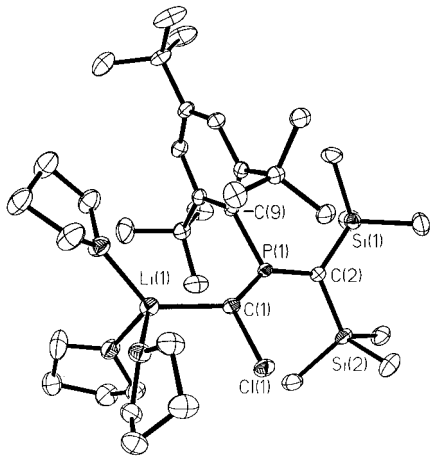

Figure 2. ORTEP view (50% probability ellipsoids, H atoms omitted for clarity) of the molecular structure of **10** in the crystal. Important bond distances and angles are listed in Table 2.

phosphoranes Mes*P(═E)═CH{Li(THF)$_n$}, (E = NMes* (**18**), C(SiMe$_3$)$_2$ (**19**)),[20,25] all three solids consist of discrete monomeric units whose metal ions are solvated by three oxygen atoms of THF molecules. The metalated double bonds exhibit *Z*-configuration, allowing the metal to occupy the sterically more accessible position trans to the second double bond, while the adjacent P1−N1 double bond in **13** is *E*-configured. The trigonal planar coordination geometries of the phosphorus and the adjacent methylene carbon atoms, as well as the propeller-like twist of the individual methylene (imino) units out of the central PC$_3$ (**10**, **11**) or PC$_2$N (**13**) planes (twist angles of the methylene (imino) fragments out of the plane of the heteroallylic CPC(N) unit are 15°/22° (**10**, **11**) and 16/62°(**13**)), comprise characteristic features of bisylene phosphoranes.[29] In **13**, steric interference between the two Mes* substituents leads to a roughly orthogonal arrangement of the aromatic ring planes (interplanar angle 115°)

(29) (a) Appel, R. In *Multiple Bonds and Low Coordination in Phosphorus Chemistry*; Regitz, M., Scherer, O. J., Eds.; Thieme Verlag: New York, 1990; pp 157−219. (b) Heydt, H. In ref 29a, pp 375−391.

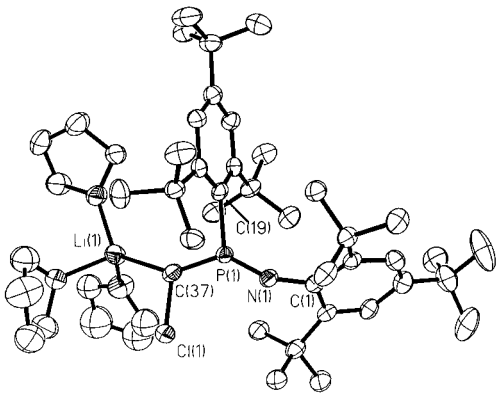

Figure 3. ORTEP view (50% probability ellipsoids, H atoms omitted for clarity) of the molecular structure of one of the two independent molecules of **13** in the crystal. Important bond distances and angles are listed in Table 2.

Table 2. Important Bond Distances (pm) and Angles (deg) for **10**−**12** (Data from Ref 21), **13**, and **15** (Data from Ref 20)

	10	**11**	**12**	**13**[c]	**15**
P1═C1[b]	166.8(2)	166.7(3)	168.2(2)	165.1(7) [164.6(7)]	167.1(6)
P1═E	169.3(2)	169.2(3)	170.0(2)	156.2(5) [156.8(5)]	167.5(5)
C1[b]−Li1	213.0(4)	213.4(7)	211.7(4)	214.4(13) [216.4(12)]	219.3(12)
C1[b]−X	181.3(2)	196.7(3)	143.8(2)	181.5(7) [181.1(7)]	181.6(6)
Li−X	321.5(6)	329.9(10)	287.1(6)	314.4(11) [312.8(11)]	296.2(11)
C1═P1═E	139.0(1)	139.8(2)	134.4(1)	131.6(3) [131.2(3)]	124.7(3)
P1═C1[b]−Li1	134.6(1)	136.9(3)	140.4(2)	138.8(5) [138.5(5)]	155.7(5)
P1═C1[b]−X	115.4(1)	114.9(2)	112.8(1)	113.3(4) [114.1(4)]	109.4(3)
Li1−C1[b]−X	109.0(1)	107.4(2)	106.1(2)	104.8(4) [103.5(4)]	94.8(3)

[a] The numbering schemes of Figures 1 and 2 are applied. [b] C37 for **13**. [c] Values for the second independent molecule are given in brackets.

and, concomitantly, to some widening of the nitrogen valence angle (138−139°), which has precedence in the structures of iminomethylene phosphoranes with comparable substitution patterns.[25,26,28,29] Comparison of the structural parameters of **10**, **11**, and **13** with those of the precursors **6**,[20] **7**,[28] and **9**[26] reveals further specific structural distortions: (i) the C1−P1−C2(N1) angles between the two double bonds at phosphorus are widened in the carbenoids by 10.9° (**6** vs **10**), 12.2° (**7** vs **11**), and 9.8 [9.4]° (**9** vs **13**); (ii) while the C1−P1 bonds are barely influenced by the metalation, the adjacent P1−C2(N1) double bonds are elongated (Δr = 3.6 (**6** vs **10**), 4.3 (**7** vs **11**), and 3.9[4.5] (**9** vs **13**) pm); (iii) the C1−P1−Li1 bond angles are substantially larger and the C1−P1−X bond angles smaller than the ideal values of 120° for an sp^2-carbon atom (see Table 2); (iv) metalation induces a marked elongation of the adjacent C−X bonds (Δr = 8.7 (**6** vs **10**), 9.1 (**7** vs **11**), and 8.2[7.8] (**9** vs **13**) pm). The latter effect is apparently compensated by a contraction of the C−Li bonds, whose distances (213.6 ± 0.6 pm, see Table 2) are shorter than in most lithium organyls (214−220 pm[13,30,31]). A more detailed discussion of the connection between structural features and bonding in phosphoranylidene carbenoids, including the previously reported data of **12** and **15**,[20,21] will be given below.

Table 3. ^{31}P and Selected ^{13}C NMR Data (−90 °C, THF/Hexane Solution) for **10**−**13** and **15**

				═**C**(Li)X		═**C**Si$_2$	
	δ ^{31}P	^2J(P,Li)	δ ^{13}C	^1J(P,C)	^1J(C,Li)	δ ^{13}C	^1J(P,C)
10	146.5	6.3	154.2	114	13.8	49.3	11.4
11	146.6	6.4	147.0	127	14.5	51.5	6.5
12	135.9[a]	7.3	221.9[b]	109	14.4	49.3	11.4
13	84.1	9.0	148.4	94	13.7		
15	165.3	5.0	165.3	111	12.0	33.5	50.7

[a] $^2J_{P,F}$ = 36 Hz, δ ^{19}F = −122.6. [b] $^1J_{F,C}$ = 371 Hz.

NMR Spectroscopic Studies. Detailed solution NMR studies of the carbenoids **10**−**13** and **15**[32] were initiated in order to characterize constitution (including determination of the degree of association) and dynamics in solution, as well as to obtain further information on the electronic structure of the π-stabilized carbenoid moiety. In view of the need for a concise specification of the metal coordination environment, experiments were performed with 99% ^{6}Li-enriched samples in nondeuterated solvents, to exploit the available information from both ^{6}Li,^{n}X spin coupling and ^{1}H,^{6}Li heteronuclear NOEs.[33] The problem of detecting ^{13}C signals of carbenoid moieties beside far more intense solvent resonances, which had been previously[13,14] overcome by employing [^{13}C,^{6}Li] doubly labeled samples, was solved by recording ^{13}C spectra with the unrefocused ^{31}P,^{13}C INEPT technique.[34] This approach combines the advantage of signal amplification by polarization transfer with the elimination of undesired signals of byproducts and solvent molecules by the applied phase cycle (if necessary, the suppression of solvent signals may be further improved by selective presaturation) and makes spectroscopic analysis of samples at natural abundance level of ^{13}C feasible. As an extra benefit, the information encoded in the antiphase structure of the signals provides an additional tool to assign the lines of overlapping multiplets and to discriminate between ^nJ(F,C) and ^nJ(P,C) couplings in **12**.

Due to the limited thermal stability of the carbenoids, NMR spectra were acquired at low temperatures between −10 and −105 °C. As anticipated, the spectra of the individual samples displayed temperature-dependent variations which are ascribable to both chemical exchange and relaxation effects.[22] To obtain reliable values, determination of chemical shifts and coupling constants was thus carried out below −70 °C in the regime of slow exchange. Relevant results are collected in Table 3. The key to the assignment of solution structures for the carbenoids **10**−**13**, **15** are the ^{31}P and ^{13}C NMR signals attributable to the atoms in the central heteroallylic unit. The resonances of the phosphorus and the silylated methylene carbon atoms (in **10**−**12**, **15**) appear in the same spectral regions as in the precursor molecules (**6**−**9**), while the signal of the metalated methylene carbon is shifted by some 90−110 ppm to lower field and lies in the range of olefinic carbon resonances. All signals of lithiated carbon atoms appear as doublets of 1:1:1 triplets due to coupling to the adjacent ^{31}P and ^{6}Li nuclei; the signal of **12** is further split by coupling with the adjacent ^{19}F nucleus (^1J(F,C) = 371 Hz). The magnitudes of ^1J(P,C) to the methylene carbon atoms are generally lower than in the precursors (^1J(P,C*XY*) = 110−127 Hz (**10**−**13**, **15**), 120−156 Hz (**6**−**9**); ^1J(P,C*Si*$_2$) = 6−11 Hz (**10**−**13**), 37−49 Hz (**6**−**9**)). A single exception from this pattern is found for **15**. Here, ^1J(P,C*Si*$_2$) is similar to that in **6** (^1J(P,C*Si*$_2$) = 48.5 Hz (**6**), 50.7 Hz (**15**)), but the coupling to the single bonded aromatic carbon atom (^1J(P,C*ipso*) = 20.2

(30) Günter, H.; Moskau, D.; Bast, P.; Schmalz, D. *Angew. Chem.* **1987**, *99*, 1242; *Angew. Chem., Int. Ed. Engl.* **1994**, *26*, 1212.

(31) Saspe, A. M.; Schleyer, P. v. R. *Lithium Chemistry—A Theoretical and Experimental Overview*; John Wiley & Sons Inc.: New York, 1995.

(32) These studies revealed some of the NMR data reported in ref 17 for **10** and **15** to be in error.

(33) See: Bauer, W. In ref 28, pp 125−172 and references cited therein.

(34) Gudat, D. *Magn. Reson. Chem.* **1993**, *31*, 925−930.

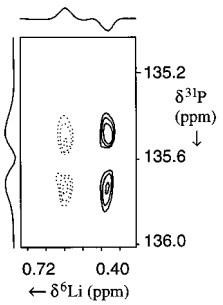

Figure 4. 2D ^{6}Li,^{31}P HMQC spectrum of **12** at −95 °C in phase-sensitive representation: positive (negative) contours are displayed as solid (dashed) lines; traces at the left and top denote projections along F1 and F2. The alignment of the two antiphase doublets parallel to F1 indicates that $|^{2}J$(F,Li)| is negligible (<0.2 Hz).

Hz) is smaller than those in both **6** (^{1}J(P,C*ipso*) = 93 Hz) and the *Z*-carbenoid **10** (^{1}J(P,C*ipso*) = 85 Hz). The multiplicities and magnitudes of *J*(C,Li) in all carbenoids resemble the patterns observed for monomeric alkyllithium derivatives with localized carbon−lithium bonds.[31,35] ^{1}H,^{6}Li HOESY spectra display cross-peaks indicating the coordination of THF molecules to the metal, while other intramolecular or intermolecular NOEs (to hexane) were absent. Altogether, these findings imply that, apart from a possible change in the number of coordinated solvent molecules, the monomeric entities with trigonal planar coordinated phosphorus atoms found in the solid state persist in solution.

Both the ^{31}P and ^{6}Li NMR spectra of the studied carbenoids revealed further residual line broadenings or multiplet structures whose interpretation as splitting by ^{2}J(P,Li) coupling was confirmed by the observation of cross-peaks in 2D ^{6}Li,^{31}P shift correlations.[36] The magnitude of these long-range couplings (5−7 Hz, see Table 3) is similar to those in lithiated bisylene phosphoranes (^{2}J(P,Li) = 5.1 Hz (**18**), 7.5 Hz (**19**)) and in HMPT adducts of lithium amides (^{2}J(P,Li) = 3−5 Hz[36]). Comparison of ^{2}J(P,Li) for pairs of *E/Z*-isomers (**10**/**15** and **13**/**17**) reveals no obvious correlation with the double bond configuration; the difference in the absolute values is similar to the difference of ^{2}J(P,H) for the diastereotopic methylene protons in Mes*P(=C(SiMe$_3$)$_2$)=CH$_2$ (^{2}J(P,H) = 4.0, 6.8 Hz[25]), but smaller than that in Mes*P(=NMes*)=CH$_2$ (^{2}J(P,H) = 4.7, 24.7 Hz[25]). A further interesting aspect is the absence of any visible ^{2}J(F,Li) coupling in both 1D ^{6}Li and ^{19}F as well as 2D ^{6}Li,^{31}P NMR spectra. The latter displays a correlation signal which appears as a pair of antiphase doublets which show the active coupling ^{2}J(P,Li) along F2 and whose relative displacement is determined by the passive couplings ^{2}J(P,F) (in F1) and ^{2}J(F,Li) (in F2). The alignment of the two components parallel to the F1 axis (see Figure 4) allows us to state that $|^{2}J$(F,Li)| < 0.2 Hz. Detailed analyses of the influence of the dynamic behavior on the NMR spectra were carried out for **12** and the pair of *E/Z*-isomers **10** and **15**. Increasing the temperature resulted for **12** in eventual collapse of all couplings to the ^{6}Li nucleus, while at the same time couplings to ^{19}F were retained. The latter rules out relaxation effects as a possible cause of this effect[19] and indicates the observed behavior to be a consequence of intermolecular exchange of Li^{+} between different carbanion fragments. The loss of couplings to the metal is further accompanied by a slight, but significant, change in the magnitudes of both ^{1}J(F,C) (−90 °C, 371 Hz; −10 °C, 365 Hz) and ^{1}J(P,C) (−90 °C, 113 Hz; −10 °C, 111 Hz).

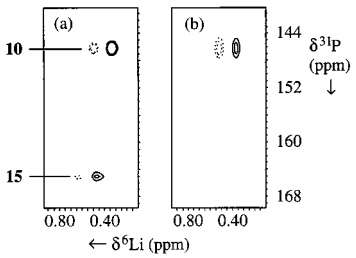

Figure 5. 2D ^{6}Li,^{31}P HMQC spectra of a mixture of the *E/Z*-isomeric carbenoids **10** and **15** at (a) −60 and (b) −40 °C. The disappearance of the cross-peak of **15** in (b) is due to the dynamic averaging of ^{2}J(P,^{6}Li) by intermolecular exchange, which is fast on the NMR time scale.

A comparable analysis of temperature-dependent effects in the spectra of the isomeric chloro-substituted carbenoids **10** and **15** revealed for **15** at temperatures above −60 °C the onset of a dynamic averaging of spin couplings to ^{6}Li similar to that for **12**, while for **10** these splittings were completely retained up to −30 °C (Figure 5). The different behavior is impressively illustrated by 2D ^{6}Li,^{31}P shift correlations of a sample containing a mixture of both isomers: while at −60 °C cross-peaks are clearly visible for both species, at −40 °C only the signal of **10** is still present, while the second peak has disappeared as a consequence of rapid intermolecular exchange.

Discussion

Crystal Structures of Carbenoids. The completion of spectroscopic and structural investigations on the series of phosphoranylidene carbenoids **10**−**13**, **15** offers for the first time the possibility for a systematic experimental study of the transmission of substituent and stereochemical influences on the bonding situation, which should yield interesting information on stabilities and reactivities of these carbenoids.

All studied compounds share common characteristic structural features which have been found previously for the vinylidene carbenoids **2** and **3**, respectively. These include the presence of longer carbon−halogen and concomitantly shorter carbon−lithium bonds than in corresponding metal-free bisylene phosphoranes and simple vinyllithium compounds, respectively, and further the widening of the P=C−Li and contraction of the P=C−X valence angles with respect to the ideal values of 120°. On the whole, these effects indicate a marked degree of rehybridization at the carbenoid carbon center.

In view of the fact that quantum chemical studies predict an increasing stability of a carbenoid if the halogen is changed from fluorine to iodine,[8,37] one might anticipate that the *E*-configured carbenoids **10**−**12** display a gradual change in the bonding situation, which is accompanied by concomitant bond deformations in the sense of the structure correlation principle of Bürgi and Dunitz.[19] A comparison of the actually observed bonding parameters of **10**−**12** suggests, however, that this is not the case. Apart from the difference in carbon−halogen distances, which matches the difference in covalence radii between Cl and Br (15 pm), the bonding parameters in the Cl- and Br-substituted carbenoids **10** and **11** deviate only insignificantly (see Table 2). The fluorocarbenoid **12** displays a further escalation of the angle distortion at the carbon atom which may be ascribed in accord with Bent's rule to the still higher electronegativity of the halogen. Regarding the rather short contacts between the fluorine and two carbon atoms in the

(35) Günther, H. In *Advanced Applications of NMR to Organometallic Chemistry*; Gielen, M., Willem, R., Wrackmeyer, B., Eds.; Wiley: New York, 1996; pp 247−290.

(36) Romesberg, F. E.; Bernstein, M. P.; Gilchrist, J. H.; Harrison, A. T.; Fuller, D. J.; Collum, D. B. *J. Am. Chem. Soc.* **1993**, *115*, 3475−3483.

(37) Schoeller, W. W., personal communication.

adjacent trimethylsilyl group (F1···C6/C7 309/319 pm) and the contraction of the P1−C1−Si2 angle in **12** (114.1(1)°) as compared to those of the heavier homologues (**10**, 118.1(1)°; **11**, 118.9(2)°), part of this deformation may also be attributed to the formation of weakly attracting hydrogen bond-like F···H_3C interactions. On the other hand, the elongation of the C−F bond with respect to a standard bond distance (r(C═C−X) = 134.0 (F), 173.4 (Cl), 188.3 pm (Br)[38]) in **12** (7.0%) is more pronounced than that in **10** (4.6%) or **11** (4.5%), and at the same time the Li···F contact amounts to 86% of the sum of the van der Waals radii and is thus slightly closer than those in **10** and **11** (r(Li···X) = 90% of the sum of van der Waals radii). Both trends indicate some weakening of the C···X and strengthening of the Li···X interactions in **12** as compared to **10** and **11** and suggest that **12** has proceeded further on its way toward fragmentation into a lithium halide and a carbene and should thus be the less stable carbenoid.

Comparison of the structural data of the carbenoids **10** and **13**, which differ in the composition of the E−P−C heteroallylic π-system, reveals as a most striking feature a contraction of the P═C(carbenoid) double bond, together with a marked deformation of the phosphorus bond angles. These variations have precedence in the structural data of known iminomethylene phosphoranes and are attributable to the combined effects of different polarization of the π-electron system and different steric interactions between substituents.[24,26] The deviations of C−Cl and C−Li bond distances at the carbenoid center in **13** from the corresponding bonds in **10** are insignificant, but a further increase in P═C−Li and decrease in P═C−Cl bond angles with respect to **12** also induces some shortening of the Li···X contact. It is not clear if this effect is of electronic (rehybridization) or steric origin (different steric interactions between the large substituents at phosphorus and carbon).

More substantial differences than those between **10**−**13** show up in a structural comparison of the *Z*- and *E*-isomers **10** and **15**. Whereas changes in the environment at the phosphorus atom remain moderate, the deviation between the P═C−Li and P═C−Cl angles is further drastically aggravated and the Li−C1 bond becomes longer (see Table 2). Surprisingly, the latter effect is not compensated by a decrease in the C−Cl distance, which is essentially identical in both compounds. While it is not clear how far the angular deformation is caused by rehybridization (i.e., a further shift of carbon s-electron density from the C−Cl into the C−Li bond), or by increased steric interference between the adjacent bulky Li(THF)$_3$ and $SiMe_3$ substituents, the trends in the bond distances suggest that the carbenoids can be formulated as contact ion pairs between a halogenated carbanion and a solvated lithium cation, as was suggested on the basis of both theoretical and experimental studies for the phosphavinylidene carbenoid **3**.[22,39] As was found there, the C−Li interaction is then merely a coordinative bond whose lengthening appears to have only limited consequences for the bonding in the remaining carbanion fragment.

Static and Dynamic NMR Parameters. The hypotheses on the bonding situation in phosphoranylidene carbenoids are further supported by the observed trends in NMR chemical shifts and coupling constants. If we adopt the description of the carbenoids as a carbanion−lithium contact ion pair, formal replacement of one halogen atom in the precursors **6**−**9** by a metal atom reduces to conversion of a strongly bonding σ-orbital into a weakly bonding orbital which has very much the characteristics of a formal lone pair at carbon engaged in a coordinative bond to an acceptor.[39] This effect depresses the energy of the magnetically allowed $\sigma-\pi^*$ electronic transition from this lone pair into the empty heteroallyllic π^*-orbital and is expected to induce a strong paramagnetic shielding contribution at the carbon atom where the lone pair is centered, but a much less pronounced effect at the phosphorus atom. The stronger deshielding in the *E*- (**15**) than in the *Z*-isomer (**10**) agrees with the longer C−Li distance in the former, which indicates a further bond weakening and concomitantly lower $\sigma-\pi^*$ transition energy. Part of the overall deshielding contribution in both isomers should also be attributable to the concurrent weakening of the remaining C−X bonds, which should result in lower σ(C−X)$-\pi^*$ and $\pi-\sigma^*$(C−X) transition energies as compared to those of **6**−**9**.

The C−Li bond lengthening in the *E*-isomer **15** as compared to those in the *Z*-isomers **10**−**13** may as well held responsible for the decrease of both ^1J(C,Li) and ^2J(P,Li) in this case. Comparison of the ^1J(P,C) couplings to the second ylene and aromatic carbon atoms in **10** and **15** reveals further a marked orientation dependence: the substituent trans to the lithium atom displays a smaller coupling than the cis substituent, regardless of the bond order (formal single or double bond). If one assumes a positive value for ^1J(P,C),[40] then the observed pattern matches the known trend that the reduced coupling ^1K(A,B) in a structure where the AB bond is adjacent to an atom with a lone pair changes to more positive (negative) values, depending on whether the lone pair is cis (trans) to the AB bond.[41] In this sense, the orientation dependence of ^1J(P,C) supports further the assumption of a formal lone pair character of the Li−C bonding orbital.

In addition to the analysis of the static NMR parameters, the dynamic exchange of metal cations between different carbanion fragments in **12** and **15** provides a direct visualization for the proposed formulation of phosphoranylidene carbenoids as contact ion pairs between α-halogenated carbanions and lithium cations. The temperature-dependent change in ^1J(F,C) and ^1J(P,C) for **12** suggests further that a partial dissociation of the contact ion pair into a solvent-separated ion pair may occur at higher temperatures. In addition to underlining that the *E*-carbenoid **15** is kinetically less stable than the *Z*-isomer **10**, the temperature-dependent changes in the ^{6}Li,^{31}P 2D spectra substantiate further the configurational stability of the anion [Mes*P(═C($SiMe_3$)$_2$)═C$^{(-)}$Cl], since any inversion at the carbanionic center would necessarily lead to interconversion of **10** and **15**, which contradicts the experimental findings. The lower *kinetic* stability of **15** allows further a consistent rationalization for the different reaction behavior of the isomers **10** and **15** which had been noted previously:[20] while **15** cyclizes above −10 °C under formal loss of LiCl and shift of one trimethylsilyl substituent to afford the phosphirene **20**, the *Z*-isomer **10** gives the CHCl-substituted bisylene phosphorane **21** as the main product, presumably via deprotonation of a solvent molecule (Scheme 5). The easier elimination of LiCl from **15** is easily explained if one assumes that the intermolecular exchange of Li^+ is, as in the case of **12**, accompanied by partial dissociation into a solvent-separated ion pair, and this suggests that **15** is not only the kinetically but also the thermodynamically (toward fragmentation into a carbene) less stable isomer.

(38) *International Tables for Crystallography*; Wilson, A. J. C., Ed.; Kluwer Academic Publishers: Dordrecht 1992; Vol. C, pp 680ff.

(39) A similar description of a coordinative C−Li bond in 2-lithio-1,3-dithianes was obtained from the interpretation of deformation electron densities, see: Amstutz, R.; Dunitz, J. D.; Seebach, D. *Angew. Chem.* **1981**, *93*, 487−488; *Angew. Chem., Int. Ed. Engl.* **1981**, *20*, 54.

(40) Dixon, K. R. In *Multinuclear NMR*; Mason, J., Ed.; Plenum Press: New York, 1987; pp 369−402 and cited literature.

(41) Gil, V. M. S.; von Philipsborn, W. *Magn. Reson. Chem.* **1989**, *27*, 409−430.

Scheme 5

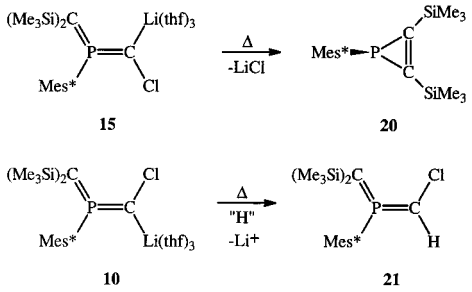

Comparison between Phosphavinylidene and Phosphoranylidene Carbenoids. Comparison of the structural data of the chlorocarbenoids **10** and **15** with those of the phosphavinylidene derivative **3**[22] exhibits similar characteristic distortions in the environment of the carbenoid center for both types of compounds. A quantitative inspection reveals that the C−Cl bond lengthening and the asymmetry between the P═C−Li and P═C−Cl bond angles in **3** (P−C 177.8(2) pm, P═C−Li 122.4 (1)°, P═C−Cl 120.5(1)°[22]) are slightly less pronounced, but on the whole very similar, as in the *Z*-phosphoranylidene carbenoid **10**. Structural data of the *E*-isomer of **3** are not available, but comparison of the ab initio calculated structures[22] of the model compounds *E/Z*-[H_3C−P═C(Cl){Li(dme)$_2$}] indicates a similar increase in bond distortions to that observed between **10** and **15**.

Quite interestingly, the structural analogies between the two sets of stereoisomers are matched by a similar analogy in chemical reactivities: for both phosphavinylidene and phosphoranylidene carbenoids, the isomer with the larger geometric distortions reacts easily under elimination of LiCl and substituent shift to afford either a phosphaalkyne[42] or a phosphirene,[20] whereas the other isomer fails to give a similar reaction. Considering further that both phosphavinylidene and phosphoranylidene carbenoids can be described as tight ion pairs of a solvated Li^+ and a carbanion,[22] it can be concluded that, despite the substantial difference in electronic structures of phosphaalkenes and bisylene phosphoranes,[29] the structure, bonding, and reactivity of the carbenoid moiety in both types of compounds are very similar.

Conclusions

Interpretation of structural and spectroscopic parameters of the carbenoids **10**−**13** and **15** provides detailed insight into the bonding situation of these systems. In particular, structure correlations indicate that, even if the F-substituted carbenoid appears to be somewhat less stable than the corresponding Br- and Cl-substituted congeners, the formal exchange of halogens induces no continuous increase in stability. Both structural and spectroscopic data support the formulation of the studied phosphoranylidene carbenoids as contact ion pairs of solvated Li^+ cations and carbanions. Comparison of the structural features of phosphavinylidene and phosphoranylidene carbenoids suggests that, despite the substantial difference in electronic structures of phosphaalkenes and bisylene phosphoranes, the bonding situation and reactivity of the carbenoid moieties in both types of compounds are very similar. Investigation of the dynamic behavior in solution allows us to visualize further a marked difference in the kinetic stabilities of *E*- and *Z*-isomers, which provides an explanation for the observed difference in reaction behavior. Beside underlining the power of NMR methods for a concise characterization of structure *and* dynamics of molecular systems in solution, this finding emphasizes that understanding of the dynamic behavior may be of essential importance for the derivation of structure−activity relations which will allow in the future a more precise understanding of the physical properties and reactivities of phosphoranylidene and other carbenoids.

(42) (a) Yoshifuji, M.; Niitsu, T.; Inamoto, N. *Chem. Lett.* **1988**, *10*, 1733. (b) Yoshifuji, M.; Kawanami, H.; Kawai, Y.; Yasunami, M.; Niitsu, T.; Inamoto, N. *Chem. Lett*. **1992**, 1053. (c) Yoshifuji, M.; Ito, S.; Toyota, K.; Yasunami, M. *Bull. Chem. Soc. Jpn.* **1995**, *68*, 1206.

Experimental Section

General. All manipulations were carried out under a dry argon atmosphere using standard Schlenk techniques. [^{6}Li]-*n*-BuLi was prepared as described in ref 14. ^{1}H, ^{31}P{^{1}H}, ^{13}C{^{1}H}, and ^{6}Li NMR spectra (300.13, 121.5, 75.5, and 44.2 MHz) were recorded on a Bruker AMX 300 instrument equipped with three independent rf channels and a triple-resonance probe head designed for BB observation and simultaneous ^{1}H and ^{31}P decoupling, and ^{19}F NMR spectra were recorded on a DRX 500 spectrometer (470.6 MHz). WALTZ-16 composite pulse decoupling with a decoupler field strength of 2.5 kHz was used for ^{1}H decoupling. NMR spectra of carbenoids were recorded in situ in the reaction mixture using samples prepared from [^{6}Li]-*n*-BuLi. ^{13}C NMR spectra of these samples were recorded with the ^{13}C,^{31}P-{^{1}H}-INEPT technique under additional suppression of strong solvent signals by selective presaturation.[34] Two-dimensional ^{1}H,^{6}Li HOESY and ^{6}Li,^{31}P polarization-transfer experiments were conducted using previously published pulse sequences.[33−36] Chemical shifts are referenced to external 85% H_3PO_4 (^{31}P), Me_4Si (^{13}C, ^{1}H), or 70% LiBr in D_2O (^{6}Li); positive values denote shifts to higher frequencies. Electron ionization (70 and 24 eV) mass spectra were run on a VG 12-250 instrument. Melting points are uncorrected.

Preparation of Compound 7. To a stirred solution of 2.17 g (5 mmol) of **4** and 2.53 g (10 mmol) of $CHBr_3$ in 30 mL of *n*-hexane was added at 0 °C 5.60 g of KOtBu. After 15 min, the mixture was allowed to warm to 25 °C and then filtered, and the precipitate was washed several times with fresh *n*-hexane. The filtrate was concentrated and left for crystallization at −25 °C. Compound **7** was isolated as orange crystals: 2.77 g (91%); mp 127−129 °C. ^{31}P NMR (THF): δ = 136.9. ^{1}H NMR (C_6D_6): δ = 7.69 (d, 2 H, ^4J(P,H) = 5.0 Hz, aryl-H), 1.84 (d, 18 H, ^5J(P,H) = 0.7 Hz, *o*-^{t}Bu), 1.30 (s, 9 H, *p*-^{t}Bu), 0.65 (s, 9 H, $SiMe_3$), 0.12 (s, 9 H, $SiMe_3$). ^{13}C{^{1}H} NMR (C_6D_6): δ = 155.5 (d, ^2J(P,C) = 7.6 Hz, *o*-aryl), 154.9 (d, ^4J(P,C) = 3.0 Hz, *p*-aryl), 126.0 (d, ^3J(P,C) = 13.0 Hz, *m*-aryl), 122.9 (d, ^1J(P,C) = 91.9 Hz, *ipso*-aryl), 60.2 (d, ^1J(P,C) = 48.5 Hz, P*C*Si$_2$), 57.3 (d, ^1J(P,C) = 120.9 Hz, P*C*Br$_2$), 40.6 (d, ^3J(P,C) = 2.7 Hz, *o*-CMe_3), 35.6 (d, ^5J(P,C) = 1.1 Hz, *p*-CMe_3), 34.5 (s, *o*-CCH_3), 31.4 (s, *p*-CCH_3), 5.3 (d, ^3J(P,C) = 5.0 Hz, Si*C*$_3$), 4.5 (d, ^3J(P,C) = 5.0 Hz, Si*C*$_3$). MS (70 eV): *m/z* (relative intensity) 606 (6) [M^+], 591 (15) [M^+ − Me], 527 (30) [M^+ − Br], 73 (100) [$SiMe_3^+$]. $C_{26}H_{47}Br_2PSi_2$ (606.13): found, 606.1300; calcd, 606.1291.

Preparation of Compound 8. To a solution of 2.85 g (15 mmol) of titanium tetrachloride in 40 mL of THF was added 0.57 g (15 mmol) of LAH at 0 °C. After being stirred for 30 min, the black suspension was cooled to −78 °C, and 2.17 g (5 mmol) of **4** and 2.06 g (15 mmol) of $CFCl_3$ were added. The reaction mixture was then stirred for 15 min at −78 °C and then allowed to warm to room temperature. After removal of the solvent in vacuo, 40 mL of *n*-pentane was added. The resulting suspension was filtered and washed several times with fresh *n*-pentane. Removal of the solvent in vacuo afforded 2.76 g of crude **8** (yield 95%) as a yellow oil, which was used for the subsequent metalation without further purification. ^{31}P NMR (THF): δ = 94.8. ^{1}H NMR (C_6D_6): δ = 7.70 (d, 2 H, ^4J(P,H) = 5.0 Hz, aryl-H), 1.85 (d, 18 H, ^5J(P,H) = 0.7 Hz, *o*-^{t}Bu), 1.29 (s, 9 H, *p*-^{t}Bu), 0.55 (s, 9 H, $SiMe_3$), 0.15 (s, 9 H $SiMe_3$). ^{13}C{^{1}H} NMR (C_6D_6): δ = 156.5 (dd, ^2J(P,C) = 7.3 Hz, ^4J(F,C) = 2.7 Hz, *o*-aryl), 155.2 (d, ^4J(P,C) = 3.4 Hz, *p*-aryl), 135.7 (dd, ^1J(F,C) = 330.0 Hz, ^1J(P,C) = 165.2 Hz, P*C*ClF), 125.8 (d, ^3J(P,C) = 13.4 Hz, *m*-aryl), 118.3 (dd, ^1J(P,C) = 98.0 Hz, ^3J(F,C) = 1.9 Hz, *ipso*-aryl), 44.3 (dd, ^1J(P,C) = 37.4 Hz, ^3J(F,C) = 8.0 Hz, P*C*Si$_2$), 40.7 (d, ^3J(P,C) = 2.7 Hz, *o*-CMe_3), 35.6

(d, ^5J(P,C) = 1.1 Hz, *p*-CMe_3), 34.4 (s, *o*-CCH_3), 31.3 (s, *p*-CCH_3), 4.3 (d, ^3J(P,C) = 4.2 Hz, SiC_3), 3.9 (dd, J = 4.9 Hz, 6.5 Hz, SiC_3). MS (70 eV): *m*/*z* (relative intensity) 500 (1) [M^+], 485 (3) [M^+ − Me], 564 (2) [M^+ − Cl], 73 (100) [$SiMe_3^+$].

General Procedure for the Preparation of Carbenoids 10−13. One millimole of the appropriate bisylene phosphorane (**6**−**9**) was dissolved in 3 mL of THF. After the mixture was cooled to −78 °C, 0.7 mL of *n*-BuLi in *n*-pentane (c = 1.6 mol L^{-1}) was added via syringe. ^{31}P and ^{6}Li NMR spectroscopic assay confirmed the formation of mixtures of the stereoisomeric carbenoids **10**/**15**, **11**/**16**, **12** (no stereoisomer assigned with certainty), **13**/**17** in approximately 6:1 molar ratios. The major products **10**−**13** were characterized in these solutions by multinuclear NMR spectroscopy. The solutions were concentrated in vacuo and left for crystallization at −25 °C. Compounds **10**−**13** were isolated as yellow or orange crystals.

Compound 10. ^{31}P{^{1}H} NMR (THF, −90 °C): δ = 146.5 (t, ^2J(P,^{6}Li) = 6.3 Hz). ^{6}Li{^{1}H} NMR (THF, −90 °C): δ = 0.4 (d, ^2J(P,^{6}Li) = 6.5 Hz). ^{1}H NMR (THF, −90 °C): δ = 7.21 (2 H, aryl-H), 0.23 (s, 9 H, $SiMe_3$), −0.37 (s, 9 H, $SiMe_3$); *o*-and *p*-^{t}Bu are concealed by solvent signals. ^{13}C{^{1}H} NMR (THF, −90 °C): δ = 154.2 (dt, ^1J(P,C) = 113.8 Hz, ^1J(C,^{6}Li) = 13.8 Hz, P*C*ClLi), 154.1 (s, *o*-aryl), 149.0 (s, *p*-aryl), 131.0 (d, ^1J(P,C) = 85.8 Hz, *ipso*-aryl), 122.8 (d, ^3J(P,C) = 9.7 Hz, *m*-aryl), 49.3 (d, ^1J(P,C) = 11.4 Hz, P*C*Si_2), 40.8 (s, *o*-CMe_3), 36.1 (s, *p*-CMe_3), 34.3 (s, *o*-CCH_3), 33.2 (s, *p*-CCH_3), 5.5 (br, SiC_3), 4.0 (br, SiC_3).

Compound 11. ^{31}P{^{1}H} NMR (THF, −90 °C): δ = 146.6 (t, ^2J(P,^{6}Li) = 6.4 Hz). ^{6}Li{^{1}H} NMR (THF, −90 °C): δ = 0.2 (d, ^2J(P,^{6}Li) = 6.4 Hz). ^{1}H NMR (THF, −90 °C): δ = 7.21 (2 H, aryl-H), 0.23 (s, 9 H, $SiMe_3$), −0.37 (s, 9 H, $SiMe_3$); *o*-and *p*-^{t}Bu are concealed by solvent signals. ^{13}C{^{1}H} NMR (THF, −90 °C): δ = 154.3 (d, ^2J(P,C) = 3.1 Hz, *o*-aryl), 150.5 (s, *p*-aryl), 147.0 (dt, ^1J(P,C) = 127.0 Hz, ^1J(C,^{6}Li) = 14.5 Hz, P*C*BrLi), 132.5 (d, ^1J(P,C) = 83.2 Hz, *ipso*-aryl), 123.5 (d, ^3J(P,C) = 9.2 Hz, *m*-aryl), 51.5 (d, ^1J(P,C) = 6.5 Hz, P*C*Si_2), 40.0 (s, *o*-CMe_3), 35.5 (s, *p*-CMe_3), 34.3 (s, *o*-CCH_3), 31.2 (s, *p*-CCH_3), 6.3 (d, ^3J(P,C) = 1.9 Hz, SiC_3), 4.7 (br, SiC_3).

Compound 12. ^{31}P{^{1}H} NMR (THF, −90 °C): δ = 135.9 (dt, ^2J(P,F) = 36.1 Hz, ^2J(P,^{6}Li) = 7.3 Hz). ^{6}Li{^{1}H} NMR (THF, −90 °C): δ = 0.5 (d, ^2J(P,^{6}Li) = 7.3 Hz). ^{19}F{^{1}H} NMR (THF, −90 °C): δ = −122.6 (d, ^2J(P,F) = 36.1 Hz). ^{1}H NMR (THF, −90 °C): δ = 7.44 (d, 2 H, ^4J(P,H) = 2.6 Hz, aryl-H), 0.12 (d, 9 H, J(F,H) = 1.2 Hz) $SiCH_3$), −0.40 (s, 9 H, $SiCH_3$); *o*-and *p*-^{t}Bu concealed by solvent signals. ^{13}C{^{1}H} NMR (THF, −90 °C): δ = 221.9 (ddt, ^1J(F,C) = 370.8 Hz, ^1J(P,C) = 109.1 Hz, ^1J(C,^{6}Li) = 14.4 Hz, P*C*FLi), 156.2 (s, *o*-aryl), 151.0 (s, *p*-aryl), 127.3 (dd, ^1J(P,C) = 80.3 Hz, ^3J(F,C) = 7.0 Hz, *ipso*-aryl), 123.5 (d, ^3J(P,C) = 9.9 Hz, *m*-aryl), 49.3 (d, ^1J(P,C) = 11.4 Hz, P*C*Si_2), 40.4 (s, *o*-*C*Me_3), 35.4 (s, *p*-*C*Me_3), 34.8 (s, *o*-*CC*H_3), 31.3 (s, *p*-*CC*H_3), 4.8 (d, J(F,C) = 6.1 Hz, $SiCH_3$), 6.5 (br, SiC_3). ^{29}Si{^{1}H} NMR (THF, −90 °C): δ = −8.4 (d, ^2J(P,Si) = 10.3 Hz), −13.0 (d, ^2J(P,Si) = 7.9 Hz).

Compound 13. ^{31}P{^{1}H} NMR (THF, −90 °C): δ = 84.1 (t, ^2J(P,^{6}Li) = 9.0 Hz). ^{6}Li{^{1}H} NMR (THF, −90 °C): δ = 0.6 (d, ^2J(P,^{6}Li) = 9 Hz). ^{1}H NMR (THF, −90 °C): δ = 7.33 (d, 2 H, ^4J(P,H) = 1.2 Hz, P-aryl-H), 6.99 (s, 1 H, N-aryl-H), 6.81 (s, 1 H, N-aryl-H); *o*-and *p*-^{t}Bu concealed by solvent signals. ^{13}C{^{1}H} NMR (THF, −90 °C): δ = 148.4 (dt, ^1J(P,C) = 93.8 Hz, ^1J(C,^{6}Li) = 13.8 Hz, P*C*ClLi), 130.9 (d, ^1J(P,C) = 67.9 Hz, *ipso*-aryl); further signals of Mes* units could not be assigned with certainty.

Preparation of Compound 15. A ^{6}Li-doped sample of the carbenoid **15** was generated via Li/H exchange from **14** as reported previously[20] and characterized by NMR spectroscopy without further workup. ^{31}P{^{1}H} NMR (THF, −90 °C): δ = 165.3 (t, ^2J(P,^{6}Li) = 5.0 Hz). ^{6}Li{^{1}H} NMR (THF, −90 °C): δ = 0.6 (d, ^2J(P,^{6}Li) = 5.0 Hz). ^{13}C{^{1}H} NMR (THF, −90 °C): δ = 165.3 (dt, ^1J(P,C) = 111.1 Hz, ^1J(C,^{6}Li) = 12.0 Hz, P*C*ClLi), 151.7 (d, ^2J(P,C) = 3.8 Hz, *o*-aryl), 149.3 (s, *p*-aryl), 130.1 (d, ^1J(P,C) = 20.2 Hz, *ipso*-aryl), 123.1 (d, ^3J(P,C) = 8.1 Hz, *m*-aryl), 38.7 (s, *o*-*C*Me_3), 35.9 (s, *p*-*C*Me_3), 33.5 (d, ^1J(P,C) = 50.7 Hz, P*C*Si_2), 33.2 (s *o*-*CC*H_3), 30.3 (s, *p*-*CC*H_3), 4.0 (br, SiC_3), 3.4 (br, SiC_3).

X-ray Crystallographic Studies of 10, 11, and 13. The structures were solved by direct methods (SHELXS-97).[43] The non-hydrogen atoms were refined anisotropically on F^2 (SHELXL-97).[43] H atoms were refined using a riding model. In **10** two THF groups and in **13** a THF group and a *p*-^{t}Bu group are disordered. An extincion correction was applied in **10** and **11**. Further details are given in Table 1.

Acknowledgment. Financial support by the Deutsche Forschungsgemeinschaft and the Fonds der Chemischen Industrie is gratefully acknowledged. This work is dedicated to Professor Dr. Joachim Bargon on the occasion of his 60th birthday.

Supporting Information Available: Full tables of crystal data, final atomic coordinates, anisotropic thermal parameters, complete positional parameters, and bond distances and angles for **10**, **11**, and **13** (PDF). This material is available free of charge via the Internet at http://pubs.acs.org.

JA990074E

(43) (a) Sheldrick, G. M. SHELXS-97. *Acta Crystallogr.* **1990**, *A46*, 467−473. (b) Sheldrick, G. M. SHELXL-97; Universität Göttingen, Germany, 1997.